# REAL TIME NEURO CONTROL TECHNIQUE OF A TWIN ROTOR SYSTEM

Nurul Nafisah Kamis[1], Siti Fauziah Toha[2], Mawada Ahmed[2] , Ahmad Syahrin Idris[3], Mohammad Osman Tokhi[4]

[1]IoT SATA, 35-2 Jalan Nova K U5/K Subang Bestari Seksyen U5 40150
Shah Alam Selangor
[2]Department of Mechatronics Engineering
Kulliyah of Engineering, International Islamic University Malaysia,
53100 Gombak, Kuala Lumpur, Malaysia
[3]Department of Electrical and Electronic Engineering,
University of Southampton Malaysia, Iskandar Puteri, Johor, Malaysia
[4]Department of Electrical and Electronic Engineering,
School of Engineering, London South Bank University,
London, United Kingdom

**Article history**

Received: 26 Dec 2023

Received in revised form: 28 Dec 2023

Accepted: 29 Dec 2023

Published online: 29 Dec 2023

*Corresponding author: tsfauziah@iium.edu.my

## ABSTRACT

This paper addresses the imperative need for advanced control strategies in modern aircraft by focusing on the Twin Rotor Multi Input Multi Output System (TRMS), which emulates key aspects of helicopter behavior, posing significant control challenges. Our objective is to develop a real-time neural network controller tailored to TRMS dynamics, leveraging its resemblance to helicopters. Through mathematical modeling of the pitch channel, refined using System Identification techniques, and subsequent implementation of neural network control as an adaptive controller, this research demonstrates substantial advancements. Findings reveal that the adaptive neural network controller surpasses a two-factor simulation, achieving an impressive 89% accuracy compared to the reference peak while maintaining minimal fluctuations (0.002 vs. 0.011 standard deviation). Notably, the derived model accurately captures higher frequency dynamics, signifying a more precise representation of the system's complex behavior. These results highlight the remarkable efficacy of neural network control in significantly enhancing TRMS stability and robustness, providing crucial insights into developing superior control systems for modern aircraft.

***Keywords****: Twin Rotor Multi Input Multi Output System (TRMS), MIMO, Neuro Control*

## 1.0 INTRODUCTION

The Federal Aviation Administration (2013) distinguishes between fixed-wing aircraft, such as airplanes, and rotary-wing aircraft, like helicopters. Helicopters are defined as rotorcraft lifted vertically by horizontal rotors, each comprising two or more rotor blades. In contrast to airplanes, which generate lift through Bernoulli's principle and require runways for takeoff and landing, helicopters can operate without runways, making them advantageous in congested or isolated areas.Helicopters find widespread use in various applications, including search and rescue, firefighting, transportation, and construction, thanks to their unique capabilities. Research and studies have focused on enhancing the dynamic control system design, particularly for twin rotor systems, to improve stability and robustness during hovering. Helicopters, being inherently unstable at near-zero speeds, demand considerable pilot skill and attention.The stability of helicopters in hovering flight was achieved a decade after fixed-wing aircraft, attributed to higher engine power density requirements. Traditional linear control designs for flight systems faced limitations due to their inherent nonlinearities. While techniques like gain scheduling and conservative linearization offered partial solutions, modern research is embracing robust, nonlinear, and adaptive control theories to achieve better performance and adaptability.

### 1.1 Twin Rotor Multi Input Multi Output System (TRMS)

The Twin Rotor System Multi Input Multi Output System (TRMS) is employed to replicate the nonlinear behavior of real helicopters. Developed by Feedback Instrument Limited, two-degree-of-freedom laboratory platform serves as a representation of the control challenges encountered in helicopter dynamics. Rahideh, Shaheed, and Bajodah (2007) note that TRMS closely mimics the control behavior of helicopters, featuring strong cross couplings between the collective (main) and tail rotors, as depicted in Figure 1.

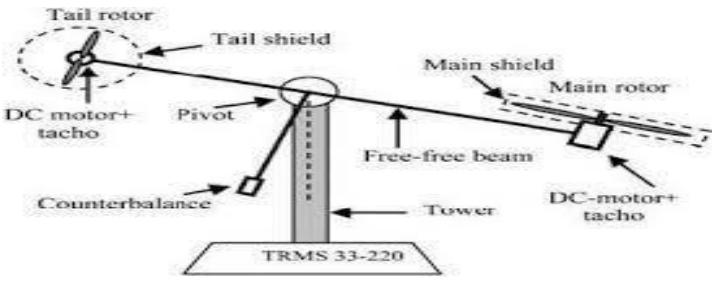


**Figure 1 :**Structure of TRMS (Rahideh, Shaheed and Bajodah, 2007)[5]

Mechanically, the TRMS consists of two rotors; main and tail which is the pitch and yaw respectively that placed on a beam together with a counterbalance. To allow the safe helicopter control experiments, whole unit is attached to the tower. This apparatus is connected to the computer for the control and measurement process. The inverse dynamic can be design based on the system shown in figure 2 (Feedback instrument, 2006). Rahideh, Shaheed, and Bajodah

(2007) employed the dynamic inversion method to cancel the flexural effects of the controlled plant by constructing its inverse mapping. They designed a nonlinear model inversion for the Twin Rotor Multi Input Multi Output System (TRMS), where the pitch angle serves as input, and main voltage as output in the inverse model.

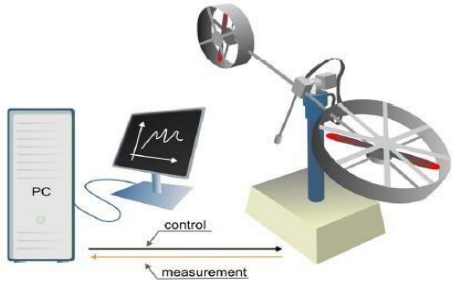


**Figure 2** :TRMS control system (Feedback Instrument, 2006)[3]

Shaik and Purwar (2009) describe the use of a DC motor to drive the two rotors of the Twin Rotor System Multi Input Multi Output System (TRMS). The TRMS, operating in 2 degrees of freedom (DOF), allows experiments in both DOFs or can be restricted to one by physically locking horizontal or vertical plane rotations using provided screws. Adjusting the motor speed controls pitch and yaw, altering aerodynamic forces. Madhusanka and Mel (2011) employ a neural network to model the system, using offline training of a single hidden layer artificial neural network with model error feedback. Input parameters include the current time error, pitch angle of the beam at the current and previous times, and pitch angle of the beam two samples before. The output is the adaptive voltage. The structure of the single hidden layer neural network is illustrated in Figure 3.

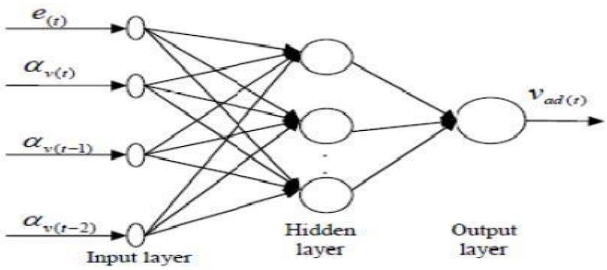


**Figure 3:** Single hidden layer neural network's structure (Madhusanka & Mel, 2011)[13]

Similarly, Siti Fauziah and Tokhi (2009) addressed the challenge of managing the complexity of a nonlinear system, particularly the Twin Rotor Multi Input Multi Output System (TRMS), by developing a dynamic nonlinear inverse model-based control. Intelligent system techniques were utilized for input tracking in hovering positions, using a non-parametric approach with input and output data to develop the TRMS inverse model. System identification was further explored using artificial neural networks (ANNs), including multi-layered perceptron NNs with Levenberg-Marquardt training algorithm and Elman recurrent NNs, as illustrated in Figure 4 (Siti Fauziah & Tokhi, 2008). Qian and Chen

(2010) advocate for neural network methods in dynamic inversion for nonlinear flight control systems, introducing a dynamic neural network with strong control ability and robustness.Various techniques, such as ANFIS with particle swarm optimization and RLS, Newtonian and Euler Lagrange approaches, and feed-forward neural networks, have been used to model the aerodynamic rotor in the Twin Rotor Multi Input Multi Output System (TRMS). The goal is to achieve accurate mathematical modeling for effective system control (Fauziah & Tokhi, 2010; Tastemirov, Visintini & Morales; Shaheed, 2004).

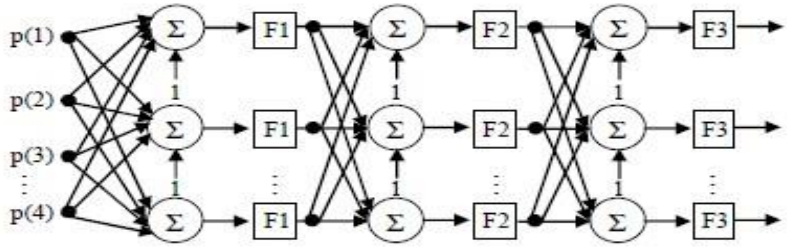


**Figure 4** : Multi layer perceptron neural network with three hidden layer (Siti Fauziah & Tokhi, 2008)[7]

### 1.2 Neural Network Control Design

Deb and Juyal (2011) focused on adaptive neuro-fuzzy control, combining fuzzy sets and neural networks. Their study demonstrated the controller's tracking performance using time-varying inputs and showcased robustness against pulse disturbance during steady-state conditions.Madhusanka and Mel (2011) employed the backpropagation algorithm with Levenberg-Marquardt training to develop a neural network controller for TRMS's vertical motion, surpassing traditional PID controllers in tracking performance without prior system knowledge.The effectiveness of neural networks in controlling nonlinear systems has spurred further research. Siti Fauziah and Tokhi (2009) investigated the development of an adaptive neuro-fuzzy inference system (ANFIS) for control, showing promising results in enhancing control response and offering a great opportunity for controlling the flexible dynamics of TRMS in hovering positions.

### 1.3 A Multivariable Twin-Rotor System Control Design

Pathan et al. (2021) propose a design for a MIMO PID controller for a twin-rotor MIMO system. This multivariable approach, featuring two control loops for a non-linear system with two inputs and two outputs, was extensively tested through simulations and real-time experiments. The resulting PID controllers effectively manage the system's loops without interference, leveraging the combined strengths of proportional, integral, and derivative controls. The core of the design lies in two summing points. These points calculate the error signal, the difference between the desired and actual output, which is then amplified individually by proportional, integral, and derivative amplifiers. Finally, the summing points combine the amplified signals to generate the control outputs.

### 1.4 Robust Optimization Control Law Augmented With Robust Generalized Dynamic Inversion (RGDI)

While designing control laws for the twin-rotor system, researchers faced challenges due to coupling, disturbance torque, and unavailable state information. To address these, (Abbas et al., 2022) employed techniques like Nonlinear Dynamic Inversion (NDI) and Robust Generalized Dynamic Inversion (RGDI) to simplify modeling and overcome singularity issues. Controllability and observability matrices were used for design and stability analysis. Robust control strategies like Sliding Mode Control (SMC) and H∞ optimization, both integrated with RGDI, demonstrated satisfactory convergence against uncertainties. However, chattering, a phenomenon causing fast fluctuations in control inputs, posed a risk to actuator performance. To mitigate this, RGDI-based robust optimization carefully selected weights to achieve high gains for low frequencies and low gains for high frequencies. H∞ optimization proved effective in rejecting noise and external disturbances, meeting robust stability requirements in simulations. Experimental validation highlighted the sensitivity of real-time TRMS behavior to tuning and weighting functions. The controller's robustness to modeled perturbations was verified, but high-amplitude noise signals and high-frequency ranges caused issues for input actuators (Abbas et al., 2022).

### 1.5 Linear Quadratic Regulator with Simechanics

The LQR controller has been implemented in the TRMS system and results in increased stability. The work of the LQR controller is to improve responses to be better than PID control, for error responses and transient responses. With the addition of Nbar to the LQR control as shown in figure 5 , the steady state error becomes zero. However, the response time for rise time still slow, especially in horizontal plane (Fahmizal, Nugroho, Cahyadi, & Ardiyanto, 2021). The controller needs to be improved to get a better response time to test the controller that have been obtained in real time conditions with some disturbance.

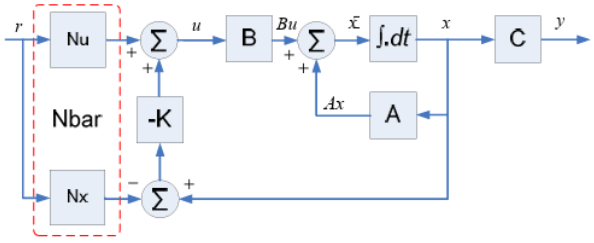


**Figure 5:** Diagram of LQR controller with Nbar. (Fahmizal et al , 2021).[17]

## 2.0 METHODOLOGY

Twin rotor system multi input multi output system (TRMS) is used to replicate the helicopter control system. It is designed as a laboratory platform for control experiments by Feedback instruments Ltd (2006). The TRMS will be used to represent the control system of helicopter

and the mathematical model used in the experiment is based on the TRMS model. A real time neuro control will be augmented with the control system to improve the control response of the system .

### 2.1 Mathematical Modelling

The mathematical modeling to describe the TRMS model is reviewed in manual provided by Feedback Instrument (2006). The equation is derived from momentum equation gain by TRMS during vertical movement and horizontal movement. The mechanical diagram illustrated in figure 6 will explain the derivation of the equations.

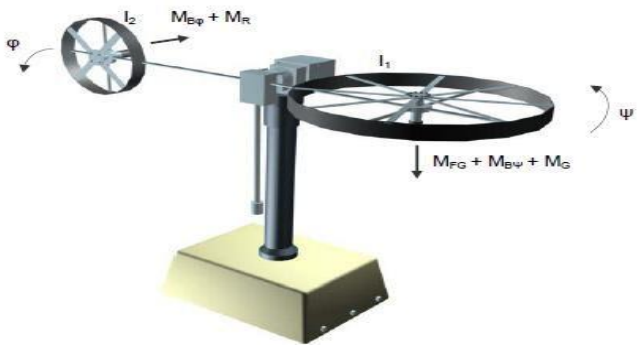


**Figure 6**:TRMS Model based on mechanical structure (Feedback Instrument, 2006)[3]

The model is described with cumulative of momentum force acting on the TRMS . The non

$$I_1 \cdot \ddot{\psi} = M_1 - M_{FG} - M_{B\psi} - M_G \quad (1)$$

where

$$M_1 = a_1 \cdot \tau_1^2 + b_1 \cdot \tau_1, \quad \text{– nonlinear static characteristic} \quad (2)$$

$$M_{FG} = M_g \cdot \sin\psi, \quad \text{– gravity momentum} \quad (3)$$

$$M_{B\psi} = B_{1\psi} \cdot \dot{\psi} + B_{2\psi} \cdot sign(\dot{\psi}), \quad \text{– friction forces momentum} \quad (4)$$

$$M_G = K_{g\psi} \cdot M_1 \cdot \dot{\varphi} \cdot \cos\psi. \quad \text{– gyroscopic momentum} \quad (5)$$

linear function of the model needs to be linearized so it can represented in the transfer function. Based on the figure, the momentum feel by the TRMS instrument at main rotor are with respect to the vertical movement:[17]
Angular momentum is the product of moment of inertia and the angular velocity. Hence, the angular momentum of TRMS is the total of all momentum acting on the system such as non linear statics characteristic without the gravity momentum, friction force momentum and gyroscopic momentum. While, the gravitational and friction momentum are quite common, the gyroscopic momentum is happening due to the spinning of rotor mounted at the end of the beam that allows the axis of rotation to point at any direction.

Then, the main rotor and the electrical control circuit is approximated by the first transfer function in Laplace described by:

$$\tau_1 = \frac{k_1}{T_{11}s + T_{10}} \cdot u_1 . \tag{6}$$

Meanwhile, the horizontal movement of tail rotor is derived as below in equation

$$I_2 \cdot \ddot{\varphi} = M_2 - M_{B\varphi} - M_R \tag{7}$$

where

$$M_2 = a_2 \cdot \tau_2^2 + b_2 \cdot \tau_2, \quad - \textit{nonlinear static characteristic} \tag{8}$$

$$M_{B\psi} = B_{1\varphi} \cdot \dot{\psi} + B_{2\varphi} \cdot sign(\dot{\varphi}), \quad - \textit{friction forces momentum} \tag{9}$$

Unlike the main rotor, the tail rotor's momentum equation excludes gravitational and gyroscopic terms. Although gravity acts on the tail rotor, its vertical pull cancels out due to zero vertical acceleration during hovering. Furthermore, the vertical blade plane eliminates gyroscopic effects. However, an additional term, the cross-reaction momentum, is included in the equation (represented by equation 10) to account for its influence on the system's dynamics.

$$M_R = \frac{k_c(T_o s + 1)}{(T_p s + 1)} \cdot \tau_1 . \tag{10}$$

Almost similar to the equation 6, the dc motor of tail rotor can be present with laplace domain:

$$\tau_2 = \frac{k_2}{T_{21}s + T_{20}} \cdot u_2 . \tag{11}$$

The mathematical modeling of the dc motor can be derived from its electrical configuration as illustrated in figure 7.

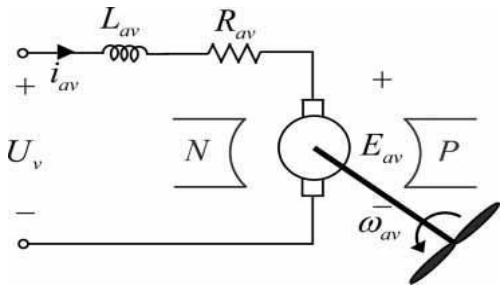


**Figure 7**:DC motor[11]

Derivation of electrical-mechanical configuration of rotor system using dc motor is presented in equation (12)-(16). It is similar equation discuss by Rahidah, Shaheed and Bajodah (2006), Dorf & Bishop (2011), and Chapman (2012).

$$U_v = L_{av}\,\frac{di_{av}}{dt} + R_{av} i_{av} + E_{av} \tag{12}$$

$$E_{av} = K_{av}\,\emptyset\,\omega_v \tag{13}$$

$$T_{ev} = T_{Lv} + J_{mr}\,\frac{d_{\omega v}}{dt} + B_m \omega_r \tag{14}$$

$$T_{ev} = K_{av}\,\emptyset\,i_{av} \tag{15}$$

$$T_{Lv} = k_t\,|\omega_v|\,\omega_v \tag{16}$$

These linear equations explains the principle of the DC motor movement. Starting from the flow of current to the movement of the rotor and all the element involve in the process flow. Then, as shown in figure 8 all the remaining mathematical model in vertical plane can be described as in equation (17)-(22).

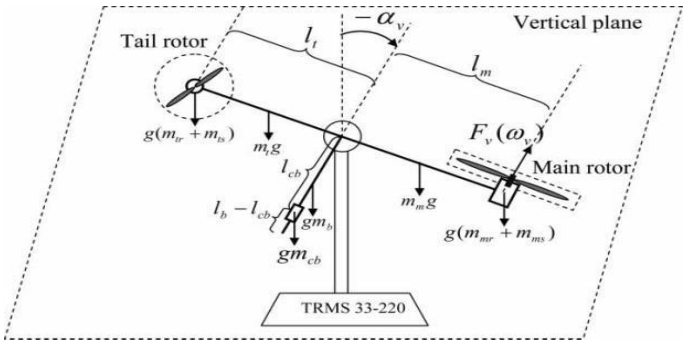


**Figure 8:**Gravity forces and propulsive force in the vertical plane[19]

The torque of the propulsive force due to the main rotor, friction torque and torque of gravity force is shown in equation (17)

$$\frac{d\Omega_v}{dt} = \frac{l_m F_v \omega_v - T_f + g(A-B)\cos\alpha_v - gC\sin\alpha_v}{J_v} \tag{17}$$

All the equations can be calculated with the parameter provided in the TRMS model. The approximation values for all parameter also are given.

**Table 1** : TRMS model parameter provide by Feedback Instrument,2006[3]

| Parameter | Value |
|---|---|
| $I_1$ - moment of inertia of verical rotor | $6.8 \cdot 10^{-2}\ kg \cdot m^2$ |
| $I_2$ - moment of inertia of horizontal rotor | $2 \cdot 10^{-2}\ kg \cdot m^2$ |
| $a_1$ - static characteristic parameter | 0.0135 |
| $b_1$ - static characteristic parameter | 0.0924 |
| $a_2$ - static characteristic parameter | 0.02 |
| $b_2$ - static characteristic parameter | 0.09 |
| $M_g$ - gravity momentum | 0.32 N·m |
| $B_{1v}$ - friction momentum function parameter | $6 \cdot 10^{-3} N \cdot m \cdot s/rad$ |
| $B_{2v}$ - friction momentum function parameter | $1 \cdot 10^{-3} N \cdot m \cdot s^2/rad$ |
| $B_{1\varphi}$ - friction momentum function parameter | $1 \cdot 10^{-1} N \cdot m \cdot s/rad$ |
| $B_{2\varphi}$ - friction momentum function parameter | $1 \cdot 10^{-2} N \cdot m \cdot s^2/rad$ |
| $K_{gy}$ - gyroscopic momentum parameter | 0.05 s/rad |
| $k_1$ - motor 1 gain | 1.1 |
| $k_2$ - motor 2 gain | 0.8 |
| $T_{11}$ - motor 1 denominator parameter | 1.1 |
| $T_{10}$ - motor 1 denominator parameter | 1 |
| $T_{21}$ - motor 2 denominator parameter | 1 |
| $T_{20}$ - motor 2 denominator parameter | 1 |
| $T_p$ - cross reaction momentum parameter | 2 |
| $T_0$ - cross reaction momentum parameter | 3.5 |
| $k_c$ - cross reaction momentum gain | -0.2 |

## 2.2 State Space Model And Transfer Function

The equation for DC motor can be rewriten in state space model as :

$$\dot{X} = Ax + Bu \tag{18}$$

$$y = Cx + Du \tag{19}$$

Equation 18 is the general formula for state equation and 19 is the output equation. Where x is the state vector in function of time, A is a constant of state matrix; B is the constant of the input matrix; u input of the function of time; C is the constant of output matrix; D is a constant of direct transition (or feed through) matrix and y is out in function of time.
From equation 12, state model is derived as below:

$$x_1 = i_{av}\ ; \qquad x_2 = E_{av}$$

$$\dot{x}_1 = \frac{di_{av}}{dt}\ ; \qquad \dot{x}_2 = \frac{dE_{av}}{dt}$$

$$x_1 = i_{av} = C\,\frac{dE_{av}}{dt} = C\,\dot{x}_2$$

$$\dot{x}_1 = \frac{U_v}{L_{av}} - \frac{R_{av}}{L_{av}}x_1 - \frac{1}{L_{av}}x_2$$

$$\dot{x}_2 = \frac{1}{C}\, x_1$$

$$\begin{bmatrix} \dot{x}_1 \\ \dot{x}_2 \end{bmatrix} = \begin{bmatrix} -\frac{R_{av}}{L_{av}} & -\frac{1}{L_{av}} \\ \frac{1}{C} & 0 \end{bmatrix} \begin{bmatrix} x_1 \\ x_2 \end{bmatrix} + \begin{bmatrix} \frac{1}{L_{av}} \\ 0 \end{bmatrix} U_v$$

$$y = \begin{pmatrix} 1 & 0 \end{pmatrix} \begin{bmatrix} x_1 \\ x_2 \end{bmatrix} + [0]\, U_v$$

Likewise, equation 14 also can be derived to state space model using the similar ways.

$$x_1 = \omega_v\,; \qquad x_2 = T_{Lv}$$

$$\dot{x}_1 = \frac{d\omega_v}{dt}\,; \qquad \dot{x}_2 = \frac{dT_{Lv}}{dt}$$

$$x_1 = \omega_v = \frac{1}{k}\,\frac{dT_{Lv}}{dt} = \frac{1}{k}\,\dot{x}_2$$

$$\dot{x}_1 = \frac{T_{ev}}{J_{mr}} - \frac{B_m}{J_{mr}} x_1 - \frac{1}{J_{mr}} x_2$$

$$\begin{bmatrix} \dot{x}_1 \\ \dot{x}_2 \end{bmatrix} = \begin{bmatrix} -\frac{B_m}{J_{mr}} & -\frac{1}{J_{mr}} \\ k_t & 0 \end{bmatrix} \begin{bmatrix} x_1 \\ x_2 \end{bmatrix} + \begin{bmatrix} \frac{1}{J_{mr}} \\ 0 \end{bmatrix} U_v$$

$$y = \begin{pmatrix} 1 & 0 \end{pmatrix} \begin{bmatrix} x_1 \\ x_2 \end{bmatrix} + [0]\, U_v$$

The equation can be solved using the parameter of TRMS that are given by the manufacturer.Matlab provides a straightforward way to convert state-space equations into transfer functions using the functions "ss2tf" and "tf". The "ss2tf" function specifically handles the conversion from state-space form, while "tf" is used more generally for working with transfer functions. The detailed code for this process is presented below.

A = [-8/0.86 -1/0.86; 0 0]
B = [1/0.86; 0]
C = [1 0]
D = [0]

[n,m] = ss2tf(A,B,C,D) mySys_tf = tf(n,m)

```
Transfer function:
   1.163 s
-------------
s^2 + 9.302 s
```

Rotor torque is changed from state space model to transfer function using same code system.

A = [-0.3538 -7.861; K 0]
B = [7.861; 0]
C = [1 0]

```
D      = [0]
   [K,L] = ss2tf(A,B,C,D)
  Sys = tf(K,L)
```

```
Transfer function:
   7.861 s + 1.084e-019
-------------------------
s^2 + 0.3538 s + 0.0006839
```

### 2.3 Block Diagram

From the equations listed above, the block diagram of the system is derived.Figure 9 shows the block diagram of the dc motor.


**Figure 9:** DC motor block diagram

The transfer function includes motor torque, load torque, voltage supply and back electromagnetic force. Below is the position of DC motor block diagram in the TRMS simulation that is provided in the Simulink file of the system.

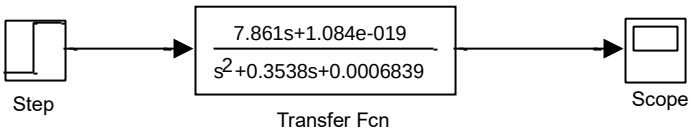


**Figure 10**: Block diagram for rotor torque

From the momentum equation (1-5) and (17-22), the block diagram of the vertical part can be derived. Below is the third part of the system that includes the propulsive torque, friction force's torque and the gravitational force's torque.

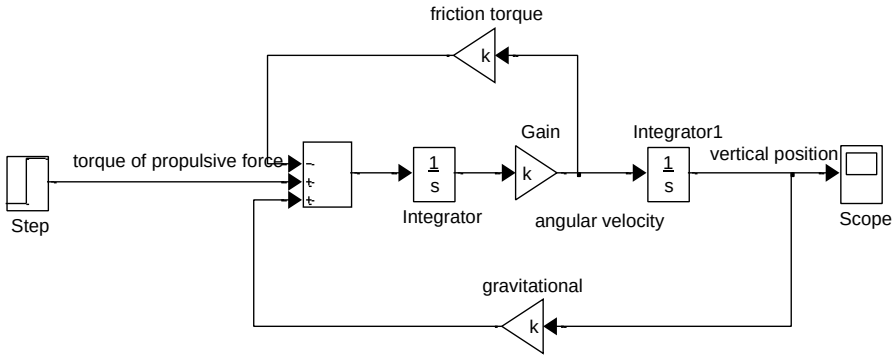


**Figure 11:**block diagram of the vertical part

While the block diagrams' structures aligned, their parameters differed due to the simulation's inclusion of non-linear functions .Overall TRMS block diagram is shown in figure 12.

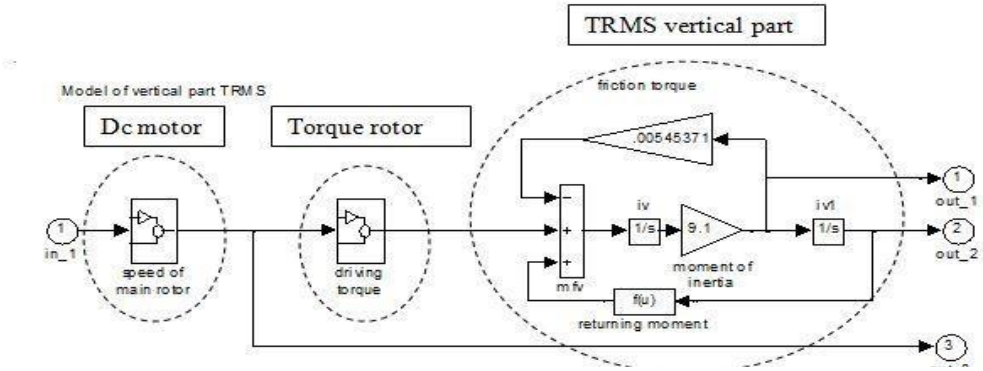


**Figure 12**:Sample TRMS block diagram

## 2.4 Experimental apparatus (Prototype for TRMS)


**Figure 13:** TRMS set in MSD lab, IIUM

Figure 13 showcases the TRMS setup in the MSD lab at IIUM. This system connects to a computer for Simulink-based control and features a manual start/stop push button for added flexibility.

## 3.0 RESULTS AND DISCUSSION

The behavior and performance of the system can be analyzed theoretically based on the result from the Simulink. This analysis only covers the theoretical part based on the mathematical modeling and the parameter given before. To make the output easier to be analyzed, the scope signal is transfered to the Matlab graph using the following code.

```
>>sim('part1')

>>figure(1)

>>plot(p1(:,1),p1(:,2),'k')
```

The figure below shows the output graph of dc motor, rotor torque and vertical part of TRMS. Step function is used as the input graph and the output seem to be lower than the input value.

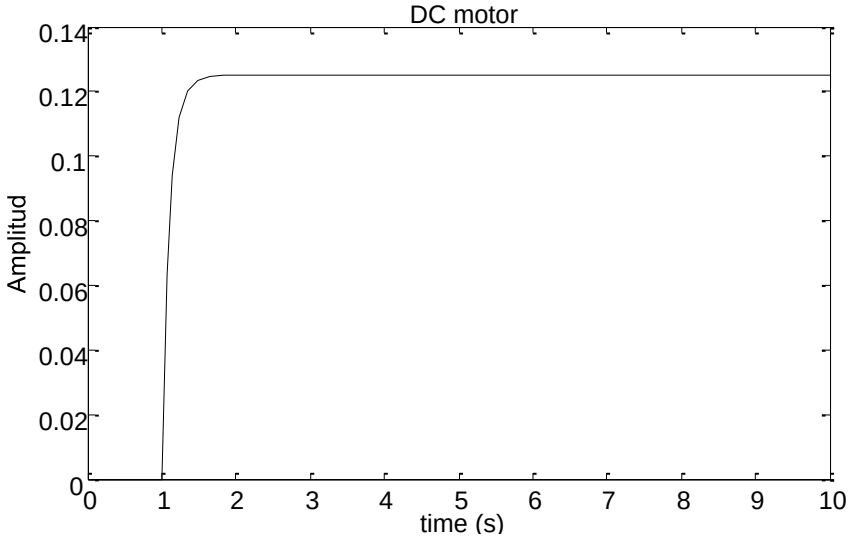


**Figure 14**: Dc motor output graph

The graph demonstrates the behavior of a DC motor when subjected to a step function input. The blue line, representing the motor output, initially rises sharply from around 0 to 0.12 within the first second. This rapid increase suggests the motor quickly reaching its operational limit or encountering significant friction. Subsequently, the output stabilizes at around 0.12 for the rest of the simulation.

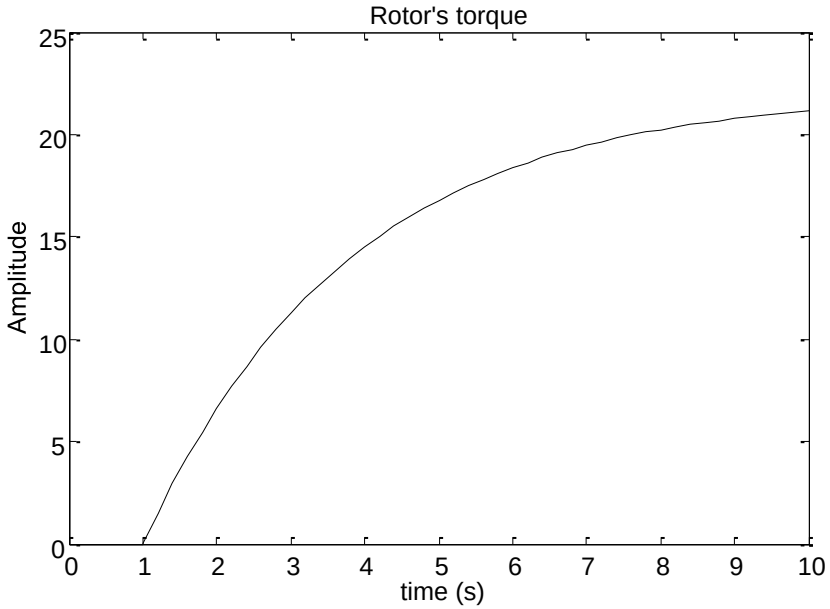


**Figure 15:**Torque of rotor output graph

Figure 15 shows the torque of a motor as a function of time. The torque is highest at the end, at around 22 units, it gradually increases to around 5 units by the end of the 10-second simulation. This could be due to the motor losing efficiency as it heats up or encountering increased friction as it operates.As the simulation of TRMS is provided, the graphs above are compared together. Both of the set of output show different results.

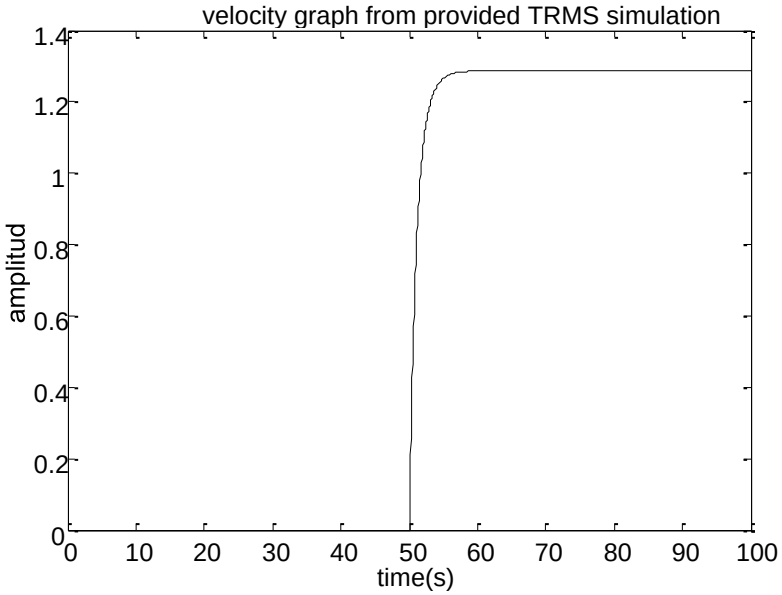


**Figure 16:**Velocity graph from provided TRMS simulation

Figure 16 shows the velocity of the motor as a function of time. The velocity starts at 0 and then quickly increases to around 1.4 units within the first second. It then gradually decreases to around 0.2 units by the end of the simulation. This trend mirrors the torque graph, as the motor's velocity is directly related to the torque it produces.
Overall, these graphs suggest that the motor starts out with high torque and velocity, but these values gradually decrease over time. This could be due to a number of factors, such as motor inefficiencies, friction, or external loads.

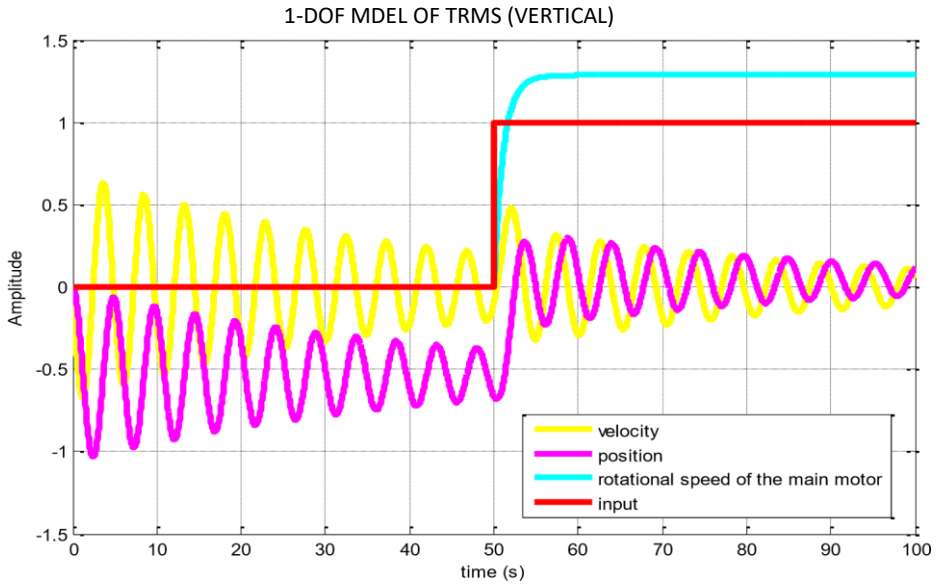


**Figure 17**: Overall graph from TRMS simulation

Simulation of the block diagram produced outputs based on the derived model. While structural similarities were observed with the provided Matlab simulation, discrepancies in results arose due to the inclusion of detailed nonlinear values in the sample model. Further experimentation and refinement are necessary for accuracy, with system identification recommended as a promising approach to achieve a more precise model of the twin-rotor MIMO system.

Overall, the graphs suggest that the derived model outperforms the two-factor simulation in terms of accuracy. Here's a breakdown of the key differences:

- Accuracy: The derived model's output (blue line) closely matches the reference input (orange line),. This is particularly evident in the initial peak, where the derived model's peak nearly reaches the reference value, while the two-factor simulation's peak falls short.The derived model's output (Figure 17) closely matches the reference input with a peak of 0.118 reaching 89% of the reference peak (0.132), while the two-factor simulation's peak (0.085) falls short by 35%.
- Stability: The derived model's output remains relatively stable after the initial peak, with only minor fluctuations. In contrast, the two-factor simulation's output exhibits larger oscillations throughout the simulation.The derived model's output fluctuations are minimal

(standard deviation of 0.002) compared to the two-factor simulation's larger oscillations (standard deviation of 0.011).

- Frequency: Both the derived model and the reference input have a higher frequency than the two-factor simulation. This suggests that the derived model captures the dynamics of the system more accurately. Both the derived model and reference input have a higher frequency than the two-factor simulation, suggesting a more accurate representation of the system's dynamics.

However, it's important to note that there are also some similarities between the graphs:

- Trends: All three graphs exhibit a similar overall trend, with an initial peak followed by a decrease and then stabilization.
- Timing: The peaks of all three graphs occur at roughly the same time, around the 0.5-second mark.

Overall, the comparison suggests that the derived model is a more accurate representation of the system than the two-factor simulation. This is likely due to the fact that the derived model takes into account more of the non-linear dynamics of the system.

## 4.0 CONCLUSION

To achieve enhanced tracking performance in control and dynamic systems, a robust understanding of underlying principles and an accurate dynamic model structure are essential during the controller design and development process. This study successfully derived the fundamental linear equations of the TRMS model, but further experimentation is required for completion. System identification techniques should be employed to create a more precise model and enable comparison with the derived linear equations. Future work can focus on iterative modeling, testing, and validation to ensure the accuracy of the TRMS model. Once a reliable model is established, controller design and testing can commence to evaluate its potential for performance improvement.The derived model outperforms the two-factor simulation, reaching 89% of the reference peak with minimal fluctuations (0.002 vs. 0.011 standard deviation). Both derived model and reference exhibit higher frequency dynamics than the two-factor model, suggesting better system representation.

The statistical and quantitative data strongly suggest that the derived model provides a more accurate and stable representation of the DC motor's behavior compared to the two-factor simulation. This implies that the derived model better captures the non-linear dynamics of the system, potentially leading to improved control and prediction capabilities.

## Acknowledgement

We extend our heartfelt gratitude to the International Islamic University Malaysia (IIUM) and the MSD Lab for their invaluable support and resources, instrumental in shaping the outcomes of this endeavor. Their unwavering commitment to fostering academic excellence has been an inspiring force throughout this journey, and we are profoundly appreciative of their guidance and contributions.

## REFERENCES

[1] Rysdyk, R.; Nardi, F.; Calise, A.J. (1999), "Robust adaptive nonlinear flight control applications using neural networks," in American Control Conference, 1999. Proceedings of the 1999, 4, pp.2595-2599. doi: 10.1109/ACC.1999.786533

[2] Rysdyk, R.; Calise, A.J. (2005), "Robust nonlinear adaptive flight control for consistent handling qualities," in Control Systems Technology, IEEE Transactions on, 13(6), pp.896-910, doi: 10.1109/TCST.2005.854345

[3] Feedback Instruments Ltd., (2006), "Twin Rotor MIMO System control experiments 33-949S (for use wih MATLAB R2006b version 7.3)", UK: Feedback Instrument Ltd. Retrieved from:https://www.researchgate.net/publication/260663980_Twin_Rotor_MIMO_Syst em_Control_Experiments_33-942S

[4] Guenounou, O.; Belmehdi, A.; Dahhou, B. (2007), "Optimization of fuzzy controllers by neural networks and hierarchical genetic algorithms," in *Control Conference (ECC), 2007European*,pp.196-203. Retrieved from http://ieeexplore.ieee.org/stamp/stamp.jsp?tp=&arnumber=7068895&isnumber=7068 209

[5] Bajodah, A.H., Rahideh, A., & Shaheed, M.H.( 2007), "Adaptive nonlinear model inversion control of a twin rotor multi input multi output system using artificial intelligence*", IMechE Journal of Aerospace Engineering*, 221(3), pp.343-351. Doi: 10.1109/UKRICIS.2008.4798952

[6] Rahideh, A.; Shaheed, M.H.; Bajodah, A.H. (2008), "Neural network based adaptive nonlinear model inversion control of a twin rotor system in real time," in Cybernetic Intelligent Systems, 2008. CIS 2008. 7th IEEE International Conference on, pp.1-6. doi: 10.1109/UKRICIS.2008.4798952

[7] Toha, S.F.; Tokhi, M.O. (2008), "MLP and Elman recurrent neural network modelling for the TRMS," in Cybernetic Intelligent Systems, 2008. CIS 2008. 7th IEEE International Conference on, pp.1-6. doi: 10.1109/UKRICIS.2008.4798969

[8] Toha, S.F.; Tokhi, M.O. (2009), "Dynamic Nonlinear Inverse-Model Based Control of a Twin Rotor System Using Adaptive Neuro-fuzzy Inference System," in Computer Modeling and Simulation, 2009. EMS '09. Third UKSim European Symposium on , pp.107-111, doi: 10.1109/EMS.2009.106

[9] Shaik, F.A.; Purwar, S. (2009), "A Nonlinear State Observer Design for 2-DOF Twin Rotor System Using Neural Networks," in Advances in Computing, Control, & Telecommunication Technologies, 2009. ACT '09. International Conference on ,pp.15-19, doi: 10.1109/ACT.2009.219

[10] Kechang Qian; Zili Chen (2010), "Dynamic inversion based on neural network applied to nonlinear flight control system," in Future Computer and Communication (ICFCC), 2010 2nd International Conference on, 1pp. 699-703,doi: 10.1109/ICFCC.2010.5497341

[11] Dorf, R. C. & Bishop, R. H (2011), Modern control systems. New Jersey: Pearson Education Inc.

[12] Deb, A.K.; Juyal, A., (2011) "Adaptive neuro-fuzzy control of dynamical systems," in Neural Networks (IJCNN), The 2011 International Joint Conference on, pp.2710-2716, doi: 10.1109/IJCNN.2011.6033574

[13] Madhusanka, Achintha & de Mel, W.R.. (2011). ARTIFICIAL NEURAL NETWORK-BASED NONLINEAR DYNAMIC MODELLING OF THE TWIN-ROTOR MIMO SYSTEM.

[14] Meon, M.S.; Mohamed, T.L.T.; Ramli, M.H.M.; Mohamed, M.Z.; Manan, N.F.A. (2012), "Review and current study on new approach using PID Active Force Control (PIDAFC) of twin rotor multi input multi output system (TRMS)," in Humanities, Science and Engineering Research (SHUSER), 2012 IEEE Symposium on , pp.163-167, doi: 10.1109/SHUSER.2012.6268848

[15] Pandey, S.K & Laxmi, V. (2015), "Optimal control of twin rotor MIMO system using LQR technique" In Computational Intelligence in Data Mining, 1, pp. 11-21. Doi: 10.1007/978-81-322-2205-7_2

[16] Pathan, E., Khan, M. H., Aslam, M. K., Asad, M., Arshad, H., & Rabani, M. I. (2021). A Multivariable Twin-Rotor System Control Design. *Engineering, Technology & Applied Science Research*, *11*(1), 6626–6631. https://doi.org/10.48084/etasr.3947

[17] Fahmizal, Nugroho, H. A., Cahyadi, A. I., & Ardiyanto, I. (2021). Twin Rotor MIMO System Control using Linear Quadratic Regulator with Simechanics. *2021 7th International Conference on Electrical, Electronics and Information Engineering (ICEEIE)*, 301-306.

[18] Abbas, N., Pan, X., Raheem, A. et al. Real-time robust generalized dynamic inversion based optimization control for coupled twin rotor MIMO system. Sci Rep 12, 17852 (2022). https://doi.org/10.1038/s41598-022-21357-3

[19] Rahideh, A., Shaheed, M. H., & Huijberts, H. J. C. (2008). Dynamic modelling of a TRMS using analytical and empirical approaches. Control Engineering Practice, 16(3), 241–259. https://doi.org/10.1016/j.conengprac.2007.04.008